

Oxidation of CO in microchannels of ceramic membranes modified with oxide catalytic coatings

M. V. Tsodikov,* N. I. Laguntsov, M. I. Magsumov, P. V. Spiridonov, O. V. Bukhtenko, T. N. Zhdanova, and V. V. Teplyakov

A. V. Topchiev Institute of Petrochemical Synthesis, Russian Academy of Sciences,
29 Leninsky prosp. 119991 Moscow, Russian Federation.
Fax: +7 (095) 230 2204. E-mail: tsodikov@ips.ac.ru

Ceramic and cermet membranes containing catalytic coatings in the internal volume of their channels were obtained. A relationship between the permeability and kinetic regularities of CO oxidation describing the transmembrane flow of gases was studied. The pre-exponential factor and apparent activation energy change as the loading of the membrane channels by the catalyst proceeds. The study of gas permeability through the membranes showed that the catalyst with a loose branched surface is distributed in the membrane microchannels. The reaction rate constant increases in parallel with an increase in the relative fraction of the catalyst surface. The CO oxidation rate is assumed to depend statistically on the number of active sites, which increases with filling of the membrane channels by the catalytic material.

Key words: ceramic membrane, cermet membrane, alkoxo method, catalytic coating, oxidation, carbon monoxide, kinetics, permeability, effective cross section of pores.

Regularities of heterogeneous catalytic reactions in channels of ceramic and cermet membranes are of great interest for researchers in the area of continuously developing nanotechnology. In the general case, gas transfer in porous media occurs due to viscous, slipping, surface, and molecular flows.^{1,2} Since catalytic coatings with large specific surface have high ratios of the catalytic coating surface to the volume of transport pores of a microreactor (S/V), it can be expected that the frequency of interaction of molecules with walls of the pores increases in these systems, and catalytic reactions occur therein more intensely than in macroreactors.

Alkoxo methods forming oxide catalytic systems from colloidal solutions of metal complex precursors can be considered as promising for designing catalytic oxide coatings in channels of ceramic membranes.^{3,4}

It has previously^{5,6} been shown that a number of oxides containing transition metal ions and obtained by the alkoxo method exhibit high activity in the low-temperature oxidation of CO.

In this work, we present the results of studying the kinetic regularities of CO oxidation with air when the gas is transferred through channels of cermet and ceramic membranes, whose internal walls are modified by single-phase oxide systems $\text{Cu}_{0.03}\text{Ti}_{0.98}\text{O}_{2\pm\delta}$ of anatase structure and $0.06\text{NiO}\cdot 0.94\text{Al}_2\text{O}_3$ of spinel structure. These oxides can be used as active catalytic systems in CO oxidation when applied as powders and coatings on monoliths.^{4,6–8}

Experimental

Cermet (TrumemTM) and ceramic (BUM) microporous membranes as tubes with a diameter of 14 mm and disks with a diameter of 40 mm were used.^{9,10} The cermet membrane has a bilayer composite structure consisting of a support and supported rutile layer. The support is based on the SS316L porous stainless steel. Its thickness is 200 μm , the average pore volume is 2 μm , and the estimated specific surface is $1.5 \cdot 10^4 \text{ cm}^2 \text{ cm}^{-3}$. A thin ceramic rutile layer is 20 μm thick, its average pore volume is 0.13 μm , the estimated specific surface of the ceramic layer is $2 \cdot 10^5 \text{ cm}^2 \text{ cm}^{-3}$, the porosity is 30–35%, and the air permeability is 330–400 $\text{m}^3 \text{ h}^{-1} \text{ m}^{-2} \text{ atm}^{-1}$.

The BUM ceramic membrane is based on titanium carbide and characterized by the following parameters: average pore size $\sim 5 \mu\text{m}$, porosity $\sim 60\%$, wall thickness 3 mm, and air permeability $1500 \text{ m}^3 \text{ m}^{-2} \text{ h}^{-1} \text{ atm}^{-1}$.⁹ Its specific features are high thermal stability and a possibility of regeneration by thermal treatment or washing with acids.

The catalytic layer of a mixed metal oxide was formed in the internal volume of membrane channels using the alkoxo method. Solutions of metal complex precursors in toluene were prepared in amounts necessary to obtain oxides of specified composition, and then reagents stabilizing mother liquors were added.^{6–8}

For the formation of a copper titanate system, solutions of *n*-tetrabutyltitanium and copper stearate were used.⁶ A solution of aluminum isopropylaluminum and nickel acetylacetonate was used to form a nickel–alumina system.⁷ Mother liquors containing precursors of catalytic coatings based on metal oxides were pumped through pores of rotating membranes under argon using a vacuum pump and collecting excess solution in an intermediate vessel. Membrane samples were dried in a wet air flow,

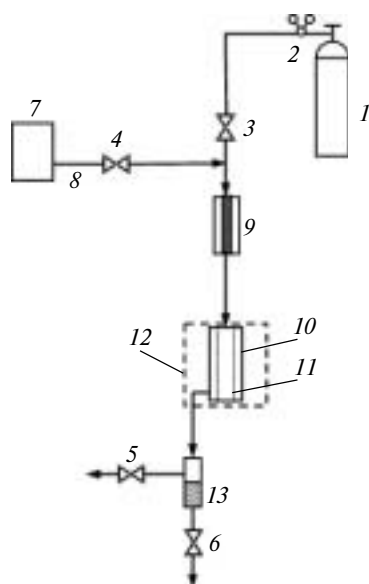


Fig. 1. Scheme of the flow-type laboratory membrane-catalytic setup for studying tubular membranes: 1, cylinder with a gaseous reactant; 2, gas reduction gear; 3–6, valves; 7, feeder; 8, liquid line; 9, furnace for preliminary heating (evaporator); 10, reactor; 11, membrane; 12, reactor furnace; and 13, separator.

evacuated at 70–80 °C, and treated for 2 h in a muffle furnace at the crystallization temperature of the oxides (450 °C). The procedure was repeated several times; the amount of a supported catalyst was monitored by the gravimetric method.

Experiments on studying the kinetic regularities of CO oxidation were carried out on laboratory flow-type catalytic setups of two types. The scheme of the flow-type membrane setup used for studying CO oxidation in tubular catalytic membranes is presented in Fig. 1. This setup simulates an enlarged laboratory setup. The cermet membrane TrumemTM was soldered with a

silver solder to tubes at the inlet and outlet of the reactor. The ceramic membrane tube was mounted in the reactor using high-temperature sealing gaskets.

Disk membranes were studied in the flow-type setup (Fig. 2) in a special diffusion cell, which was used to study simultaneously regularities of oxidation and determine the permeability of catalytic membranes.

Experiments were carried out in the regime of transmembrane transfer (filtration) of gaseous reagents through catalytic membranes produced as tubes or disks under an excessive pressure of the starting mixture of 0.11–0.15 MPa. Gas mixtures containing CO and O₂ in different concentrations (diluted with special-purity nitrogen) were fed to the internal side of the membrane.

The rate of CO oxidation was determined assuming an ideal displacement reactor

$$r = dX_i/d\tau_i, \quad (1)$$

where X_i (mol. fractions) is the conversion, and τ_i is the superficial contact time reduced to a mole of the reactant.

$$\tau_i (\text{cm}^2 \text{ h} (\text{mol CO})^{-1}) = S \cdot 22400 \cdot 100 / (60WC_{i,0}), \quad (2)$$

where $C_{i,0}$ (vol.%) is the volume concentration of the i th reagent (CO or O₂) in the initial gas mixture; S (cm²) is the geometric surface of the membrane; and W (n cm³ min⁻¹) is the volume gas flow.

The conversion is $X_i = (n_{i,0} - n_i)/n_{i,0}$, where $n_{i,0}$ and n_i are the molar fractions (volume concentration) of the reactant in the starting mixture and at the reactor outlet, respectively. The reaction order was predicted analyzing plots of the conversion vs. contact time constructed for different reaction order values ($n = 0.5, 1.0$, and 1.5).

The concentrations of CO and O₂ in the starting gas mixture and reaction products were determined using a Riken—Keike gas analyzer (Japan) equipped with an IR measuring cell and a Beckman gas analyzer (Germany) with an electrochemical cell.

The initial concentrations of CO and O₂ in model mixtures were 0.98 and 2.03 vol.%, respectively.

The gas permeability parameters were studied on a membrane diffusion cell (see Fig. 2) in a vacuum-compression regime. The pressure at the inlet (p_{in}) was maintained within 1.5–2.5 atm, and that at the outlet (p_{out}) was 0.2–0.5 atm. The permeability was calculated by the formula

$$Q = J/(\Delta p \cdot A), \quad (3)$$

where Q (nL h⁻¹ m⁻² atm⁻¹) is the gas permeability through the membrane; J (nL h⁻¹) is the gas flow through the membrane; $\Delta p = p_{\text{in}} - p_{\text{out}}$ is the pressure drop at the membrane (atm); and A (m²) is the surface area of the membrane.

Results and Discussion

Permeability and characteristics of catalytic membranes. Ceramic membranes consisting of oxide and titanium carbide are inactive in the catalytic oxidation of CO. At the same time, carbon monoxide is oxidized with a remarkable rate when the gas mixture is transferred through the membrane, whose inner pore volume contains catalytic oxide systems.

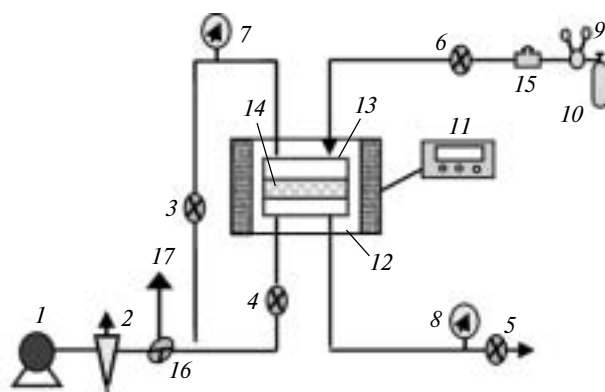


Fig. 2. Scheme of the setup for studying disk catalytic membranes at 20–1200 °C: 1, vacuum pump; 2, vacuum trap; 3–6, gas valves; 7 and 8, vacuum manometers; 9, gas reduction gear; 10, cylinder with a gas under study; 11, temperature-controlling unit; 12, furnace for heating a diffusion cell; 13, diffusion cell; 14, membrane; 15, fine adjustment valve; 16, three-way stopcock; and 17, gas outlet to analysis.

Table 1. Amount of the supported catalyst (m), specific surface (S_c), permeability, and characteristics of the catalytic coating

Type of membrane ^a	$m/\text{g cm}^{-3}$	Permeability /nL m ⁻² h ⁻¹ atm ⁻¹	Characteristics of catalyst calculated to monolith coating			Characteristics obtained from data on permeability		$S_c/\text{m}^2 \text{g}^{-1}$
			d^b	l^c	S^d/m^2	d^b	l^c	
μm			μm					
BUM (sample 1)	0.225	1142000	4.26	0.10	0.213	3.95	0.25	8.3
BUM (sample 2)	0.380	765400	4.11	0.18	0.195	3.21	0.36	13.3
BUM (sample 3)	0.700	304000	3.79	0.34	0.190	2.16	1.15	25.5
"Trumem"	0.900	240000	—	—	—	—	—	32.8

^a The catalyst is $\text{Cu}_{0.03}\text{Ti}_{0.985}\text{O}_2$.^b Pore size.^c Coating thickness.^d Internal surface.

The experimental results are presented in Table 1 along with the catalyst content in a unit volume of the membrane, permeabilities for both types of membranes, and estimated parameters of the effective cross section of ceramic membrane channels obtained from the experimental data on permeability and calculated for a monolith layer using the Hagen—Poiseuille equation¹¹ (Eq. (4)).

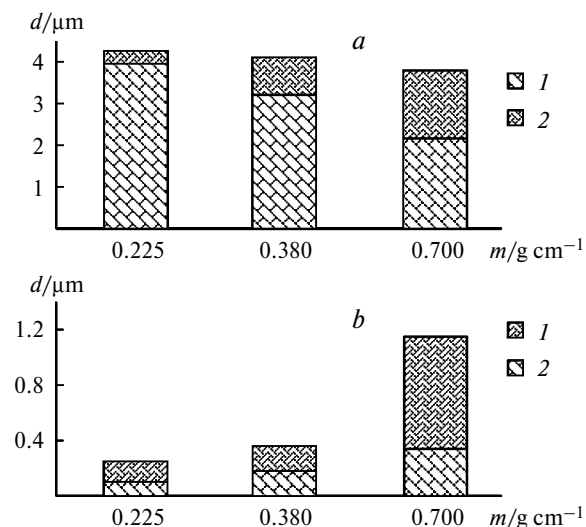
$$J = \varepsilon r^2 / (8\eta \Delta p / \Delta x), \quad (4)$$

where ε is the fraction of pores in the membrane, r is the average pore diameter, η is the dynamic viscosity of the gas mixture, and Δx is the membrane thickness.

The viscous flow regime in circular uniform capillaries was used as a model for theoretical estimation of pore sizes before and after modification of the membrane.

Comparative analysis included the measurement of air permeability of the membrane as a function of the fraction of supported catalyst. The pore radius of the modified membrane was calculated from a decrease in the flow (see Eq. (4)). The pore size (expected as calculated to the nonporous monolith catalytic coating) was estimated from the weight fraction of the catalysts uniformly introduced onto the internal walls of the membrane channels, the initial membrane porosity (35% for the membranes TrumemTM and 60% for the membranes BUM), and the physical density of copper titanate oxide (3.84 g cm^{-3}). The initial data and calculated results are presented in Table 1. The estimated specific surface areas of oxides formed in the membrane channels have been obtained previously⁵ from the BET data.

As can be seen from the data in Table 1, the pore size of the membrane microchannels decreases with an increase in the weight of supported catalyst, and the actual decrease considerably exceeds the expected value calcu-

**Fig. 3.** Change in the effective cross section of the membrane channels (*a*) and catalytic coating thickness (*b*) at different amounts of the supported catalyst: 1, experiment and 2, calculation.

lated assuming the uniform coating of membrane pores. The diagrams shown in Fig. 3 clearly demonstrate this trend: an increase in the weight of supported catalyst increases the coating thickness (decrease in the pore radius) to thicknesses much exceeding the expected values.

As follows from the data in Table 1 and Fig. 3, the real effective pore diameter obtained from the data on permeability is by 30–40% lower and the coating thickness in the internal volume of channels is much larger than it could be expected for the formation of a monolith layer.

The results obtained indicate that the catalytic layer formed in the membrane channels is, probably, a loose layer of porous oxide distributed in the internal volume

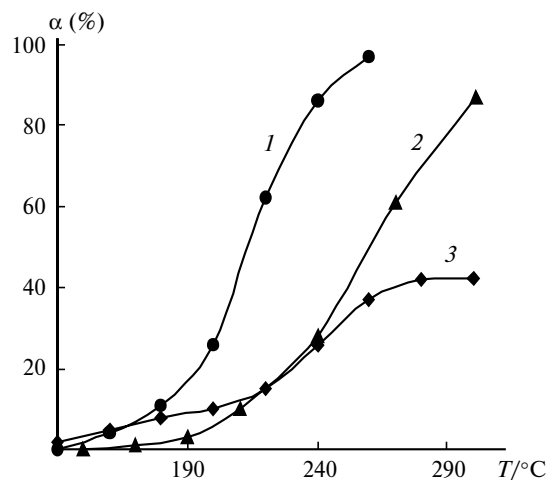


Fig. 4. Conversion of CO in oxidation vs. size of channels and reaction temperature on the cermet (1, 2) and ceramic membranes (3): $\text{Cu}_{0.03}\text{Ti}_{0.985}\text{O}_2$ (1, 3) and $\text{NiO} \cdot \text{Al}_2\text{O}_3$ (2). Sizes of channels in the initial membrane: 0.13 (1, 2) and 1 μm (3); herein after α is conversion (vol.%).

of the membrane microchannels having a developed surface.¹²

Catalytic activity. The temperature plots of the conversion of CO in oxidation for different membranes and catalysts at the same specific weight of the catalyst are shown in Fig. 4. It can be seen that the shape of curves describing the response of the CO conversion to temperature substantially depends on the nature of the oxide coating and size of channels of the membrane itself. The highest CO conversion is observed on the cermet membrane when the copper titanate system is used. It is almost an order of magnitude higher than that for the system containing the pelleted catalysts with the same composition.¹³ The CO conversion on the cermet membrane is much higher than that on the ceramic membrane, although the ratio of the length to effective diameter of channels for the cermet membrane ($l/d \approx 200$) is almost an order of magnitude lower than that for the ceramic membrane ($l/d \approx 1000$). Probably, the determining parameter is the pore size, which in the cermet membrane is by an order of magnitude lower than in the ceramic membrane. It cannot be excluded that the process is noticeably affected by the configuration of pore "branching."

It is known¹⁴ that the oxidation of CO-rich gas mixtures on catalysts containing noble metals has a negative-order dependence on CO. When the CO concentration is lower than the stoichiometric value, no reaction inhibition is observed. The linear plots of the oxidation rate vs. concentrations of CO and oxygen at different temperatures and superficial contact times suggest that the oxidation reaction has a first-order dependence on both reactants (Fig. 5).

The rate of CO oxidation on the membranes of both types modified by a catalytic coating depends substan-

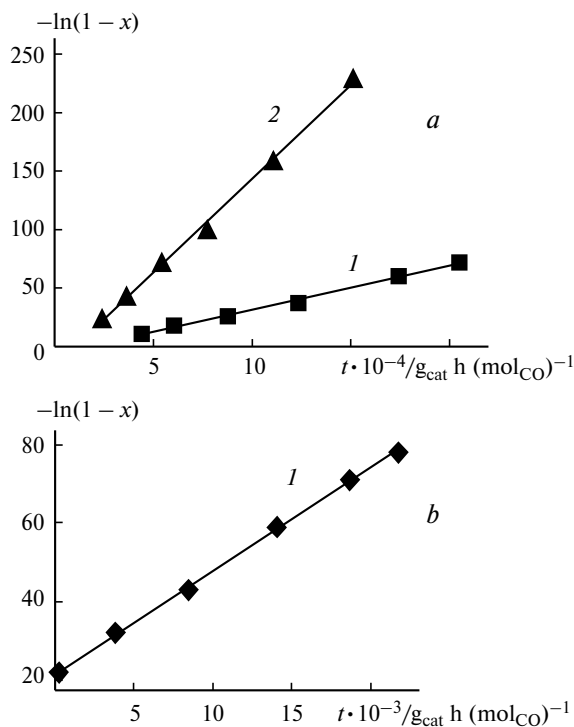


Fig. 5. Determination of the reaction order with respect to CO (a) and oxygen (b) at 190 (1) and 210 K (2); t is the superficial contact time.

tially on the superficial contact time and temperature. This indicates that the oxidation reaction occurs in the kinetic region. This assumption is completely confirmed by the linear character of the dependence of the reaction rate on the inverse temperature (Fig. 6).

The temperature dependence of the rate of CO oxidation in the membrane-catalytic module can be presented as

$$k = k_0 \exp[-E/(RT)]. \quad (5)$$

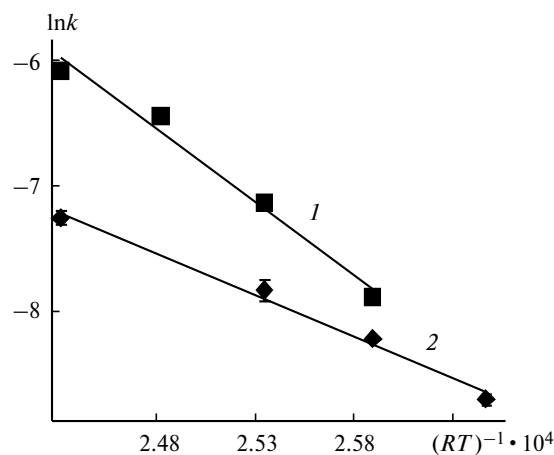
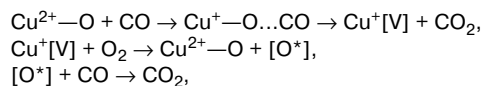


Fig. 6. Temperature plots of $\ln k$ in the Arrhenius coordinates for the cermet (1) and ceramic (2) membranes.

The CO concentration at the outlet of the membrane channels is described by the equation

$$C/C_0 = \exp\{-(k_0 C_0 \tau / 100) \exp[-E_a/(RT)]\}. \quad (6)$$

It has previously been shown by the X-ray diffraction and EXAFS methods that the catalytic systems $\text{Cu}_x\text{Ti}_{1-0.95x}\text{O}_{2\pm\delta}$ obtained by the alkoxo synthesis are single-phase oxides of anatase structure. In these structures, divalent copper ions isomorphously substitute the near-surface titanium ions to distort the tetragonal structure.⁶ According to the EXAFS and XPS data, the copper ions are typically weakly bonded to the surface O atoms. Therefore, they easily lose oxygen to be reduced to Cu^+ .⁶ Based on these data, a scheme was proposed, according to which the enhanced activity of these oxides in CO oxidation is explained by the involvement of the surface nonbridging (terminal) O atoms coordinated with the divalent copper ions



where [V] is the vacancy in the oxide lattice.

It can be assumed that the weakening of a bond between the copper ions with the surface and lattice O atoms, which is caused by the incorporation of copper into the anatase structure, is explained by an increase in tetragonal distortions in the local structure of the copper-containing polyhedron. This distortion can be a result of the Jahn–Teller effect inherent in several transition metals forming mixed oxide systems.^{15,16}

According to the presented scheme, molecular oxygen occupy vacancies in the coordination sphere of copper, resulting in the regeneration of catalytically active sites. In this case, oxygen radicals with high reactivity can be generated on the catalyst surface.

Since the rate of CO oxidation depends on the size of channels of the initial membrane (see Fig. 4), it is of interest to study the dependence of the kinetic regularities of CO oxidation on the degree of filling of the internal channel space by the catalytic coating.

The temperature plots of the conversion of CO oxidation for diffusion of the reaction gas through three disk ceramic membrane samples, which contain different amounts of the supported copper-containing catalyst and are held in the reaction cell (also designed for measuring permeability), are presented in Fig. 7. The kinetic curves of the CO conversion, calculated theoretically and obtained experimentally from Eqs (5) and (6), coincide satisfactorily (Fig. 8).

The larger the catalyst amount in the membrane, the faster the increase in the conversion with temperature. An almost 100% conversion is achieved only on sample 3

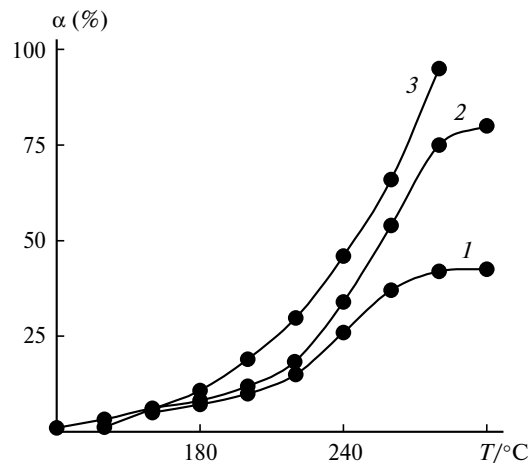


Fig. 7. Temperature plot of the conversion of CO for the ceramic membrane with different amounts of the catalyst (samples 1–3, see Table 1). The consumption of the working gaseous mixture is $5 \text{ cm}^3 \text{ min}^{-1}$.

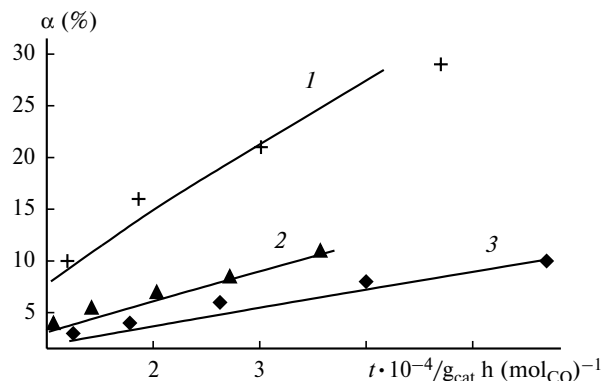


Fig. 8. Kinetic curves of CO conversion on the ceramic membrane at different temperatures and amounts of the supported catalyst: 220°C , $0.7 \text{ g}_{\text{cat}} \text{ cm}^{-3}$ (1); 220°C , $0.225 \text{ g}_{\text{cat}} \text{ cm}^{-3}$ (2); and 180°C , $0.7 \text{ g}_{\text{cat}} \text{ cm}^{-3}$ (3). Lines are calculation, and points are experiment; t is the superficial contact time.

containing the largest amount of the catalyst: 0.70 g cm^{-3} (see Figs 7 and 8).

The kinetic parameters for one cermet and three ceramic samples are presented in Table 2. The experimental data were processed at CO conversions not higher than 30%, because, as can be seen from the data in Fig. 5, for these CO conversions, the deviation from the linear dependence in the first-order coordinates does not exceed 5%.

An increase in the catalyst amount increases the pre-exponential factor by almost nine orders of magnitude, whereas the apparent activation energy increases from 30 to 116 kJ mol^{-1} .

An increase in the pre-exponential factor usually indicates an increase in the number of active sites and, correspondingly, the number of active collisions of molecules

Table 2. Kinetic parameters of CO oxidation in the membrane-catalytic module

Type of membrane ^d	<i>T</i> /°C	τ_s^a /cm ² h (mol CO) ⁻¹	α (%)	k^b mol CO/cm ² h ⁻¹ atm ⁻¹	k_0^c	E_a /kJ mol ⁻¹
BUM (sample 1)	180	32400	5.5	$1.8 \cdot 10^{-5}$	0.51	30.28
	200	36489	7.0	$2.2 \cdot 10^{-5}$		
	220	35704	11.0	$3.4 \cdot 10^{-5}$		
BUM (sample 2)	180	47280	6.0	$1.3 \cdot 10^{-5}$	33.57	47.36
	200	47104	8.0	$1.8 \cdot 10^{-5}$		
	220	42801	15.0	$3.5 \cdot 10^{-5}$		
BUM (sample 3)	180	65471	10.0	$1.7 \cdot 10^{-5}$	$1 \cdot 10^5$	67.53
	200	74146	24.0	$4.0 \cdot 10^{-5}$		
	220	50922	29.0	$7.1 \cdot 10^{-5}$		
"Trumem"	190	44075	10.2	$3.8 \cdot 10^{-5}$	$5.46 \cdot 10^9$	116
	200	38950	19.4	$8 \cdot 10^{-5}$		
	210	24088	21.4	$1.6 \cdot 10^{-4}$		
	220	19988	25.0	$2.3 \cdot 10^{-4}$		

^a Superficial contact time.^b Reaction rate constant.^c Pre-exponential factor.^d The catalyst is Cu_{0.03}Ti_{0.985}O₂.

of reacting substrates with the active surface. The explanation of a change in the activation parameter ($E/(RT)$) with an increase in the amount of catalyst of the same nature is worthy of special attention. It is seen from the data in Fig. 9 and Table 1 that the logarithm of the reaction rate constant increases in parallel with the calculated filling of the membrane channels. Since the oxidation reaction occurs in the kinetic region, it can be assumed that reactions in catalytic microchannels of the membrane represent the compensation effect that is rather rarely observed in heterogeneous catalysis.^{17–19}

It can be assumed that surface adsorption processes in micropores of the catalytic system distributed in the mem-

brane microchannels contribute to the heat effect of the reaction caused by an increase in the heat of reactant condensation. However, in this case, a increase in the amount of the catalytic system with a developed surface of mesopores in the membrane microchannels would decrease the observed apparent activation energy (E_{app}), because $E_{app} = E_{true} - \delta_{cond}$ (E_{true} is the true activation energy, and δ_{cond} is the heat of condensation in pores available for adsorption).¹⁹

It seems more probable that the equilibrium process of formation of an intermediate "activated" complex in the first step of the reaction in the membrane microchannels depends statistically on the number of active sites of the catalytic system ([cat])



An increase in the active surface area with the amount of the supported catalytic system results, probably, in an increase in the number of excited states determining the entropy factor in the Boltzmann dependence

$$\Delta S = RT \ln(L_2/L_1),$$

where L_1 and L_2 are the numbers of excited states for the formation of surface S_{surf}^1 and S_{surf}^2 , respectively, in the membrane channels.

The parallel increase in $\ln k$ and the relative surface fraction with an increase in the catalyst amount indicates indirectly that this assumption is valid (see Tables 1 and 2).

The state of a transition complex (in which a CO molecule is chemisorbed on the active sites of the surface) can be considered as the state of fluctuation of the surface energy of active sites.

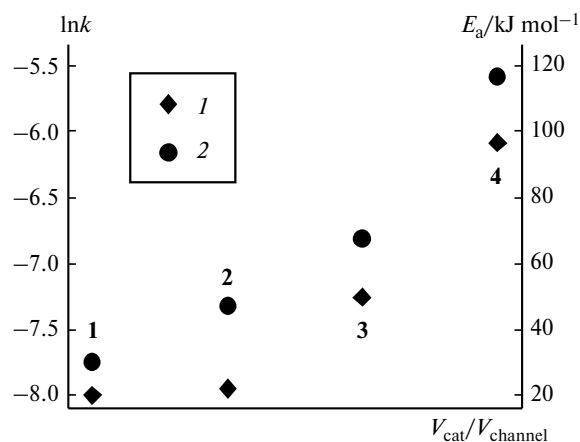


Fig. 9. The logarithm of the reaction rate constant (1) and activation energy (2) as functions of different fillings of channels of the ceramic (1–3) and cermet (4) membranes by the catalyst; $V_{\text{cat}}/V_{\text{chann}}$ is the relative fraction of filling of the membrane channels with the catalyst.

Accepting that the active sites are statistically independent, we can use the theorem on the relative fluctuation of the additive function of state for a system consisting of N independent parts

$$\delta = 1 / \sqrt{N} \sim 1/\sqrt{k_0},$$

where N is the number of active sites.^{20,21}

It is seen that if the pre-exponential factor (k_0) indirectly reflects the number of excited states (N), then the relative value of δ (δ_n/δ_1 , where n is the number of subsequent catalyst supporting procedures) characterizing the average relative energy fluctuation decreases substantially with an increase in the catalyst amount in samples 1, 2, and 3 (see Table 1), being 1, 0.123, and 0.002, respectively. This fact indicates that the statistical number of CO molecules having an energy sufficient for overcoming the potential barrier of the reaction decreases, most likely, with an increase in the amount of the catalyst distributed in the membrane channels. The latter is reflected in an increase in the activation parameter of the reaction. At the same time, the number of these collisions (or their probability) increases substantially.

This statement is confirmed by an increase in the order of the pre-exponential factor, which contributes predominantly to an increase in the oxidation rate constant.

The above assumptions explain the increase in the reaction rate with an increase in the contribution of relative volume fraction of the catalytic system in the internal volume of membrane channels, when the gas flow through the membrane is characterized, as a whole, by the viscous flow regime.

This work was financially supported by the Russian Foundation for Basic Research (Project No. 02-03-33053) and the Netherlands Organization for Scientific Research NWO (Grant 47.015.009).

References

1. S. T. Hwang and K. Kammermeyer, *Membranes in Separations*, John Wiley, New York, 1975, 452 pp.
2. S. Vilani and I. K. Kikoin, in *Obogashchenie urana [Uranium Enrichment]*, Energoatomizdat, Moscow, 1983, p. 51 (in Russian).
3. N. Ya. Turova, E. P. Turevskaya, and M. I. Yanovskaya, *The Chemistry of Metal Alkoxides*, Kluwer Academic Publishers, Amsterdam, 2001, 384 pp.
4. E. A. Trusova, M. V. Tsodikov, E. V. Slivinskii, and V. G. Lipovich, *Neftekhimiya*, 1999, **5**, 1 [*Petroleum Chemistry*, 1999, **5** (Engl. Transl.)].
5. E. A. Trusova, M. V. Tsodikov, E. V. Slivinskii, G. G. Hernandez, O. V. Bukhtenko, T. N. Gdanova, D. I. Kochubey, and J. A. Navio, *Mendeleev Commun.*, 1998, **3**, 102.
6. M. V. Tsodikov, Ye. A. Trusova, Ye. V. Slivinskii, G. G. Hernandez, D. I. Kochubey, V. G. Lipovich, and J. A. Navio, *Studies in Surface and Catalysis (Lonvain-la-Neuve, Belgium, 1998, September 1–4)*, Eds B. Delmon and J. T. Yates, Lonvain-la-Neuve, Belgium, 1998, **118**, 679.
7. M. V. Tsodikov, O. B. Bukhtenko, O. G. Ellert, D. I. Kochubey, S. M. Loktev, and S. I. Kucheiko, *Proc. 11th RISO Intern. Symp. on Metallurgy and Materials Science: Structural Ceramics — Processing, Microstructure, and Properties*, Eds J. J. Bentzen, J. B. Bilde-Sorensen, N. Christiansen, A. Horsewell, and B. Ralph, RISO National Laboratory, Roskilde, Denmark, 1990, 505.
8. M. V. Tsodikov, E. A. Trusova, Yu. V. Maksimov, G. G. Ernandes, E. V. Slivinskii, and D. I. Kochubei, *Tez. dokl. 2-go Mezhdunar. seminara "Blochnye nositeli i katalizatory sotovoi struktury" [Proc. 2nd Intern. Seminar "Monolith Supports and Catalysts of Honeycomb Structure"]* (Novosibirsk, July 12–15, 1997), Novosibirsk, 1997, 134 (in Russian).
9. L. I. Trusov, *Membrane Tech.*, 2000, No. 128, 10.
10. I. P. Borovinskaya, A. G. Merzhanov, and V. I. Uvarov, Pat. RF 2175904 of 25.02.2000; *Byul. Izobret. [Invention Bulletin]*, 2001, **32** (in Russian).
11. M. Mulder, *Basic Principles of Membrane Technology*, Center for Membrane Science and Technology, University of Twente, The Netherlands, Kluwer Academic Publishers, Dordrecht—Boston—London, 1995.
12. R. A. Kozlovskii, V. V. Yushchenko, L. E. Kitaev, O. V. Bukhtenko, A. M. Voloshchuk, L. N. Vasil'eva, and M. V. Tsodikov, *Izv. Akad. Nauk, Ser. Khim.*, 2002, 887 [*Russ. Chem. Bull., Int. Ed.*, 2002, **51**, 967].
13. G. F. Ernandez, Ph. D. (Chem.) Thesis, A. V. Topchiev Institute of Petrochemical Synthesis, Russian Academy of Sciences, Moscow, 1999, 184 pp. (in Russian).
14. O. V. Krylov and V. A. Matyshak, *Promezhutochnye soedineniya v geterogennom katalize [Intermediate Compounds in Heterogeneous Catalysis]*, Nauka, Moscow, 1965, 310 pp. (in Russian).
15. F. A. Cotton and G. Wilkinson, *Advanced Inorganic Chemistry*, Intersci. Publ., Wiley and Sons, New York—London—Sydney, 1965, 316 pp.
16. Yu. V. Maksimov, M. V. Tsodikov, E. A. Trusova, I. P. Suzdalev, and J. A. Navio, *Catal. Lett.*, 2001, **72**, 11.
17. S. Z. Roginskii, *Problemy kinetiki i kataliza [Problems of Kinetics and Catalysis]*, 1944, **6**, 9 (in Russian).
18. S. Z. Roginskii, *Geterogennyi kataliz v khimicheskoi promyshlennosti [Heterogeneous Catalysis in Chemical Industry]*, GNTIKhL, Moscow, 1955, 37 (in Russian).
19. O. M. Poltorak, *Lektsii po teorii kataliza [Lectures on the Theory of Catalysis]*, Izd. Moscow State University, Moscow, 1968, 155 pp. (in Russian).
20. V. G. Levich, *Kurs teoreticheskoi fiziki [The Course of Theoretical Physics]*, Nauka, Moscow, 1960, **1**, 910 pp. (in Russian).
21. Ch. A. Wert and R. M. Thomson, *Physics of Solids*, McCrow-Hill Book Company, New York—San Francisco—Toronto—London, 1964, 563 pp.

Received September 19, 2003;
in revised form April 27, 2004